Journal of Energy in Southern Africa 21(1): 35–51
DOI: http://dx.doi.org/10.17159/2413-3051/2010/v21i1a3248

Use of artificial roughness to enhance heat transfer in solar air heaters – a review

Thakur Sanjay Kumar
Department of Mechanical Engineering, BRCM College of Engineering & Technology, Bahal, Bhiwani (Haryana), India

N S Thakur
Department of Mechanical Engineering, National Institute of Technology, Hamirpur, Himachal Pradesh, India

Anoop Kumar
Department of Mechanical Engineering, National Institute of Technology, Hamirpur, Himachal Pradesh, India

Vijay Mittal
Department of Mechanical Engineering, BRCM College of Engineering & Technology, Bahal, Bhiwani (Haryana), India

Abstract
Improvement in the thermo hydraulic performance of a solar air heater can be done by enhancing the heat transfer. In general, heat transfer enhancement techniques are divided into two groups: active and passive techniques. Providing an artificial roughness on a heat transferring surface is an effective passive heat transfer technique to enhance the rate of heat transfer to fluid flow. In this paper, reviews of various artificial roughness elements used as passive heat transfer techniques, in order to improve thermo hydraulic performance of a solar air heater, is done. The objective of this paper is to review various studies, in which different artificial roughness elements are used to enhance the heat transfer rate with little penalty of friction. Correlations developed by various researchers with the help of experimental results for heat transfer and friction factor for solar air heater ducts by taking different roughened surfaces geometries are given in tabular form. These correlations are used to predict the thermo hydraulic performance of solar air heaters having roughened ducts. The objective is to provide a detailed review on heat transfer enhancement by using an artificial roughness technique. This paper will be very helpful for the researchers who are researching new artificial roughness for solar air heater ducts to enhance the heat transfer rate and comparing with artificial roughness already studied by various researchers.

Keywords: solar air heater, artificial roughness, active & passive technique, heat transfer, friction factor

1. Introduction

The rapid depletion of fossil fuel resources has necessitated an urgent search for alternative sources of energy. Of the many alternatives, solar energy stands out as the brightest long range promise towards meeting the continually increasing demand for energy. Solar energy is available freely, omnipresent and an indigenous source of energy provides a clean and pollution free atmosphere. The simplest and the most efficient way to utilize solar energy is to convert it into thermal energy for heating applications by using solar collectors. Solar air heaters, because of their inherent simplicity are cheap and most widely used collector devices. Solar air heaters are being used for many applications at low and moderate temperatures. Some of these are crop drying, timber seasoning, space heating, chicken brooding and curing / drying of concrete / clay building components. The thermal efficiency of solar air heaters is low due to two reasons: low ther-

mal capacity of air and a low heat transfer co-efficient between the absorber plate and air flow through duct.

In order to make the solar air heater economically more viable, their thermal efficiency needs to be improved. This can be done by enhancing the heat transfer co-efficient between the absorber plate and air flow through a duct. In general, heat transfer co-efficient enhancement techniques can be divided into two groups; namely active and passive.

The active techniques require external forces, e.g. electric field, acoustic and surface vibration. Over the past 70 years, the heat transfer enhancement by using a strong electric field has been continuously studied. The electro hydrodynamic (EHT) enhancement of heat transfer refers to the coupling of an electric field with the fluid field in a dielectric fluid medium – EHD induced secondary flow or ionic wind. This type of flow can be used not only for the pressure drop control in a flow channel but also for the enhancement of heat transfer.

The passive techniques require special surface geometries, such as rough and external surface, fluid additives and swirl flow devices i.e. twisted tap inserts to create a swirling flow. Passive techniques have being used by researchers for 140 years for increasing the heat transfer rate in a heat exchanger (Laohalertdecha, 2007).

This paper is divided in to five sections which are further divided into various subsections. Section 1 gives the introduction of solar air heaters and different heat transfer enhancement techniques. Section 2 deals with the concept of artificial roughness and a brief discussion of various roughness parameters. Section 3 deals with thermo hydraulic characteristics for a solar air heater. Section 4 deals with the comparison among various geometries by plotting the Colburn factor (j factor) and friction factor (f factor) against Reynolds number with the help of correlations developed by various researchers and finally the paper is concluded in Section 5.

2. Concept of artificial roughness

Artificial roughness is basically a passive heat transfer enhancement technique by which thermo hydraulic performance of a solar air heater can be improved. The artificial roughness has been used extensively for the enhancement of forced convective heat transfer, which further requires flow at the heat-transferring surface to be turbulent. However, energy for creating such turbulence has to come from the fan or blower and the excessive power is required to flow air through the duct. Therefore, it is desirable that the turbulence must be created only in the region very close to the heat transferring surface, so that the power requirement may be lessened.

This can be done by keeping the height of the roughness elements to be small in comparison with the duct dimensions. The key dimensionless geometrical parameters that are used to characterize roughness are:

1. Relative roughness pitch (p/e): Relative roughness pitch (p/e) is defined as the ratio of distance between two consecutive ribs and height of the rib.
2. Relative roughness height (e/D): Relative roughness height (e/D) is the ratio of rib height to equivalent diameter of the air passage.
3. Angle of attack (α): Angle of attack is inclination of rib with direction of air flow in duct.
4. Shape of roughness element: The roughness elements can be two-dimensional ribs or three-dimensional discrete elements, transverse or inclined ribs or V-shaped continuous or broken ribs with or without gap. The roughness elements can also be arc-shaped wire or dimple or cavity or compound rib-grooved. The common shape of ribs is square but different shapes like circular, semi-circular and chamfered have also been considered to investigate thermo hydraulic performance.
5. Aspect ratio: It is ratio of duct width to duct height. This factor also plays a very crucial role in investigating thermo-hydraulic performance.

3. Thermo-hydraulic characteristics for solar air heater

Nikuradse (1950) carried out experiment in order to develop velocity and temperature distribution for roughened surfaces. Webb (1971) revealed that the velocity profile in the turbulent flow region is strongly dependent upon the roughness height along with flow the Reynolds number. A correlation based on the law of wall similarity for sand grain roughness in pipes with different grades of closely packed sand roughness ($0.004 < e/d < 0.0679$) has been developed as:

$$e^+ = \frac{e}{D}\sqrt{\frac{f}{2}}\,\mathrm{Re} \qquad (2.1)$$

and

$$R(e^+) = \sqrt{2/f} + 2.5\ln\left[\frac{2e}{D}\right] + 3.75 \qquad (2.2)$$

Where e^+ is called roughness Reynolds number and R (e^+) is known as momentum transfer roughness function.

Dipprey and Sabersky (1963) have developed a relation for heat transfer in terms of a heat transfer function G (e^+), which is expressed as:

$$G(e^+) = \left[\frac{f}{2St} - 1\right]\sqrt{f/2} + R(e^+) \qquad (2.3)$$

Gee and Webb (1980) reported experimental information for a single phase forced convection in a cir-

cular tube containing a two dimensional rib roughness with a helix angle, and developed a relationship for friction roughness parameter and heat transfer roughness parameter as:

$$R(e^+) = \left[2/f + 2.5 \ln\left(\frac{2e}{D}\right) + 3.75 \right] \left(\alpha_a / 50 \right)^{0.16} \quad (2.4)$$

$$G(e^+) = \left[\frac{f/2 \cdot St - 1}{\sqrt{f/2}} + R(e^+) \right] \left(\alpha_a / 50 \right)^{J} \quad (2.5)$$

Where $J = 0.37$ for $\alpha_a < 50°$
$J = -0.16$ for $\alpha_a > 50°$

Experimental data collected by various researchers on various geometries of rib-roughened surfaces, have been utilized to develop correlation in the following form:

$$R(e^+) = R[e^+, p/e, \alpha, \text{duct shape, rib shape}] \quad (2.6)$$

$$G(e^+) = G[e^+, p/e, \alpha, \text{duct shape, rib shape}] \quad (2.7)$$

It was realized that the statistical correlations may be more suitable for design and also easy to formulate. Such relationship can be expressed as:

$$Nu = Nu[Re, e/D, p/e, \alpha, \text{Rib shape, Duct shape}] \quad (2.8)$$

$$f = f[Re, e/D, p/e, \alpha, \text{Rib shape, Duct shape}] \quad (2.9)$$

Several experimental studies of heat transfer and friction characteristics have been carried out for solar air heater applications. In solar air heaters, one broad wall of the rectangular section air flow passage is subjected to uniform heat flux, while the remaining three walls are insulated. Therefore, the solar air heaters are modelled as a rectangular channel having one rough wall and three smooth walls. This makes the fluid flow and heat transfer characteristics distinctly different from those found in the case of a channel with two opposite roughened walls, roughened annular and circular tubes.

Various researchers have investigated the effect of different roughness parameters of artificial roughness elements in thermo-hydraulic characteristics for solar air heater. The most important effect produced by the presence of a rib on the thermo-hydraulic characteristics i.e. flow pattern, is the formation of a vortex between ribs filling approximately two thirds of cavity, and energy interchange with the main flow (Karwa et al., 1999). The vortices so generated are responsible for the turbulence, which result in the desirable increase in heat transfer and the undesirable drop in pressure. The effect of different roughness parameters on thermo-hydraulic characteristics as investigated by various researchers is given below.

3.1 Relative roughness pitch (p/e)

Various researchers have shown the effect of a relative roughness pitch (p/e) on the flow pattern i.e. heat transfer coefficient and friction factor. Table 1 shows the value of relative roughness pitch (p/e) for a maximum value of a heat transfer coefficient for different types of artificial roughness. Figure 1 (Prasad & Saini, 1988) depicts the flow patterns downstream from a rib as a function of a relative roughness pitch. Due to separation at the rib, reattachment of the free shear layer does not occur for a relative roughness pitch (p/e) – less than about 8 to 10. The maximum heat transfer coefficient occurs in the vicinity of the reattachment point. For relative roughness pitch (p/e) (less than 8 to 10), reattachment will not occur, which results in the decrease of the heat enhancement rate. The rate of increase in the friction factor will increase with the decrease of pitch. However, an increase in the relative roughness pitch (p/e) beyond 10 resulted in the decrease of heat transfer enhancement.

Table 1: Values of relative roughness pitch (P/e) at which maximum value of heat transfer coefficient for different roughness geometries used in solar air heater duct

Investigators	*Roughness geometry*	*Value of relative roughness pitch at which maximum value of heat transfer coefficient (P/e)*
Prasad and Saini (1988)	Wire	10
Karwa et al. (2001)	Chamfered rib	7.09
Bhagoria et al. (2002)	Transverse wedge	7.57
Sahu and Bhagoria (2005)	90°broken transverse	13.33
Jaurker et al. (2006)	Transverse rib-grooved	6
Karmare and Tikekar (2007)	Metal grit rib roughness	17.5
Layek et al. (2007)	Transverse chamfered rib-grooved	6
Varun et al. (2008)	Combination of inclined and transverse ribs	8
Saini and Verma (2008)	Dimple-shape roughness	10

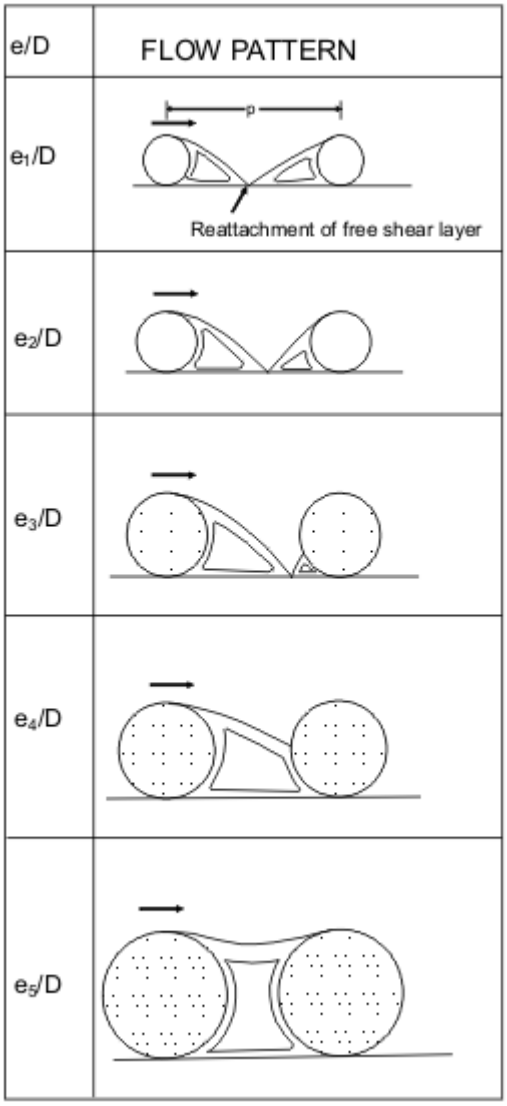

Figure 1: Flow patterns downstream of ribs with the roughness as a function of relative roughness pitch
Source: Prasad & Saini, 1988

3.2 Relative roughness height (e/D)

Figure 2 (Prasad & Saini, 1988) and Figure 3 (Prasad & Saini, 1991) depict the flow pattern downstream of a rib and effect on the laminar sub-layer as the rib height is changed respectively. Breakage of the viscous sub layer due to repeated ribs, increases the rate of heat transfer by creating local wall turbulence. If the ribs protrude beyond the viscous sub-layer, they would increase the heat transfer rate, but also cause much higher friction losses. Optimal thermo hydraulic performance conditions are obtained when the roughness height is slightly higher than the transition sub-layer thickness (Prasad & Saini, 1991).

Table 2 shows the values of the relative roughness height (e/D) for a maximum value of heat transfer coefficient.

3.3 Angle of attack

Various researchers have investigated experimentally, the effect of angle of attack on the flow pattern. Besides a relative roughness pitch and relative roughness height, the parameter that has been found to be most influential to flow pattern is the angle of inclination of the rib i.e. angle of attack of flow with respect to the rib position. The inclined rib gives a higher heat transfer rate than the transverse rib because of the secondary flow induced by the rib, in addition to breaking the viscous sub-layer and producing local wall turbulence. It is pointed out that the two fluid vortices immediately upstream and downstream of a transverse rib are essentially stagnant relative to main stream flow which raises the local fluid temperature in the vortices and wall temperature near the rib resulting in low heat transfer.

The vortices in the case of inclined ribs move along the rib so subsequently to join the main stream causing the fluid to enter near the leading end of rib and coming out near the trailing end. These moving vortices therefore bring in cooler

Table 2: Values of relative roughness height (e/D) at which maximum value of heat transfer coefficient for different roughness geometries used in solar air heater duct

Investigators	*Roughness geometry*	*Value of relative roughness height at which maximum value of heat transfer coefficient (e/D)*
Prasad and Saini (1988)	Wire	0.033
Karwa et al. (2001)	Chamfered rib	0.0441
Momin et al. (2002)	V-shaped rib	0.034
Bhagoria et al. (2002)	Transverse wedge	0.033
Jaurker et al. (2006)	Transverse rib-grooved	0.036
Karmare and Tikekar (2007)	Metal grit rib roughness	0.044
Layek et al. (2007)	Transverse chamfered	
rib-grooved	0.04	
Saini and Verma (2008)	Dimple-shape roughness	0.0379
Saini and Saini (2008)	Arc shaped wire	0.0422

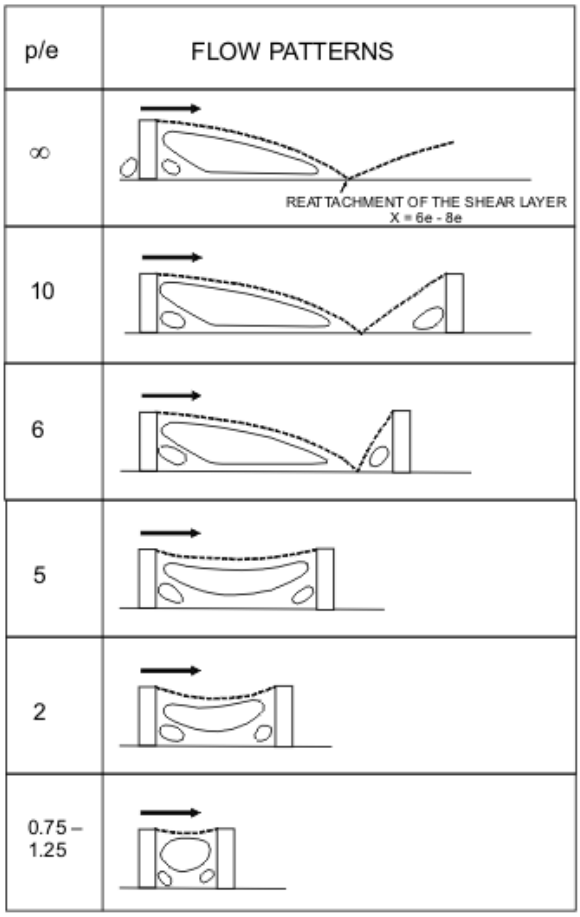

Figure 2: Flow patterns downstream of wires with the roughness as a function of relative roughness height
Source: Prasad & Saini, 1988

channel fluid in contact with leading end, raising the heat transfer rate while the trailing end heat transfer is relatively lower. This phenomenon therefore results in strong span wise variation of heat transfer.

3.4 Shape of roughness elements

Besides a relative roughness pitch, relative roughness height and angle of attack, shapes of various roughness elements also influence the heat transfer coefficient and friction factor. Different shapes of roughness elements are discussed.

3.4.1 V- shaped rib

Muluwork *et al.* (1998) have investigated the effect of a staggered discrete V- apex up and down on the thermal performance as depicted in Figure 4. The Stanton number for V-down discrete ribs was higher than the corresponding V-up and transverse discrete roughened surfaces. The Stanton number ratio enhancement was found to be 1.32 to 2.47 in the range of parameters covered in the investigation. Further for the Stanton number, it was seen that the ribbed surface friction factor for V-down discrete ribs was highest among the three configurations investigated.

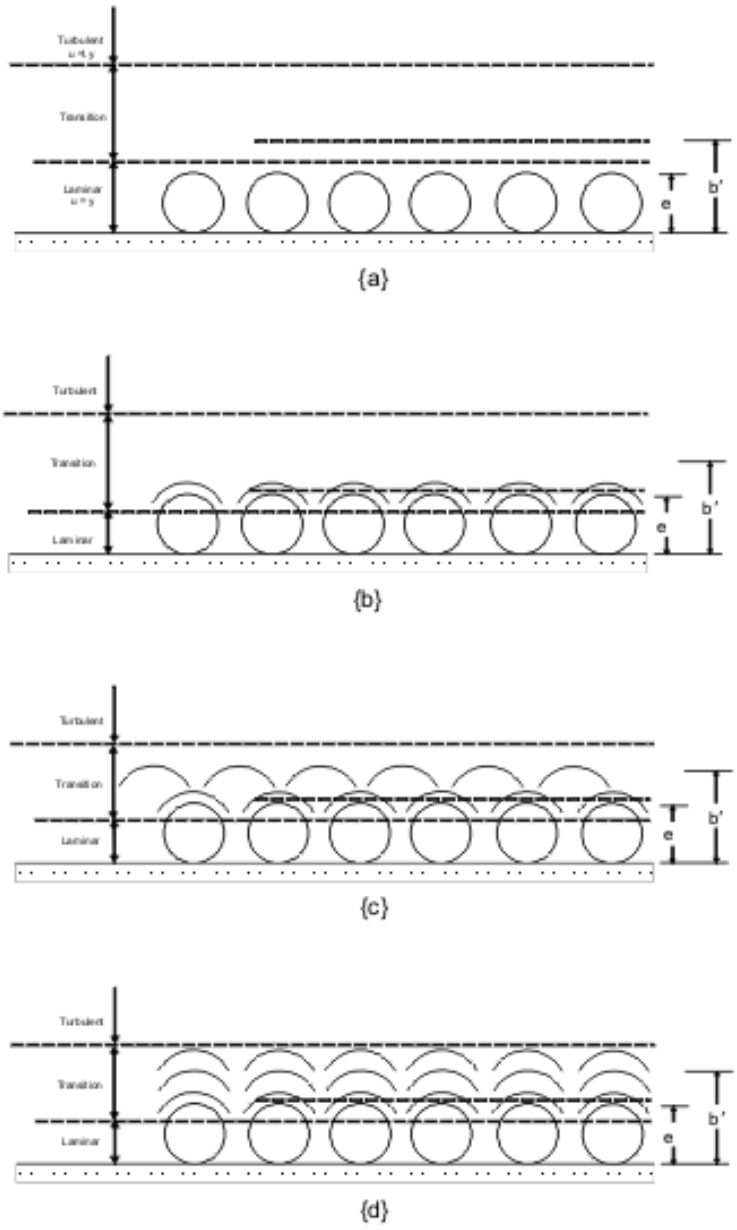

Figure 3: Roughness height with respect to laminar sub layer
Source: Prasad & Saini (1991)

Momin *et al.* (2002) has investigated the effect of relative roughness height and angle of attack for a fixed relative roughness pitch of 10 with the Reynolds number range of 2500 to 18000 for a V-shaped rib as depicted in Figure 5. It was found that the rate of increase of the Nusselt number with an increase in Reynolds number is lower than the rate of increase of the friction factor. It was found that for the relative roughness height of 0.034, the V-shaped ribs enhanced the values of Nusselt number by 1.14 and 2.30 times over inclined ribs and smooth plate.

Karwa (2003) has investigated and revealed the effect of transverse, inclined, V-continuous and V-discrete patterns on heat transfer and the friction factor in a rectangular duct. The ribs in the V-pat-

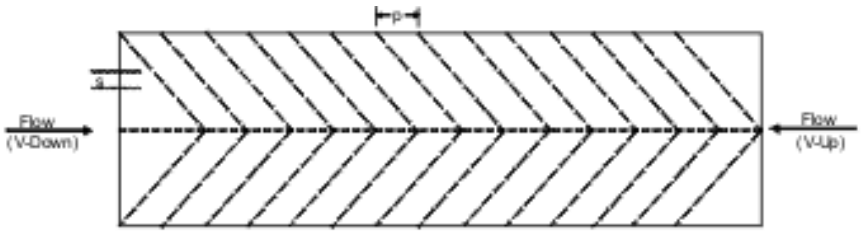

Figure 4: Type and orientation of roughness element investigated by Muluwork *et al.* (1998)

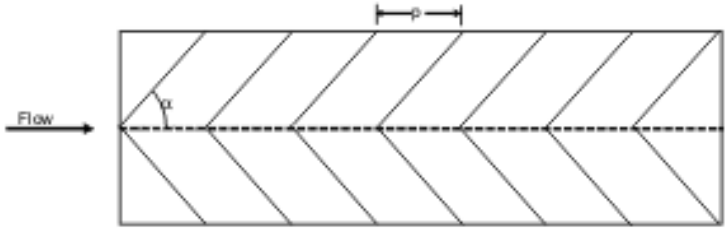

Figure 5: Type and orientation of roughness element investigated by Momin *et al*. (2002)

tern were tested for both pointing upstream (V-up) and down stream (V-down) to the flow. The angle of inclination of the ribs in inclined and V-pattern was 60˚. The enhancement in the Stanton number over the smooth duct was up to 137%, 147%, 134% and 142% for the V-up continuous, V-down continuous, V-up discrete and V-down discrete rib arrangement respectively. The friction factor ratio for these arrangements was up to 3.92, 3.65, 2.47 and 2.58, respectively. Based on the equal pumping power, V-down discrete roughness gave the best heat transfer performance.

3.4.2 Broken or discrete rib

Broken V-shaped or broken parallel ribs can create more secondary flow cells and produce more local turbulence in the opposite wall region in comparison to the continuous V-shaped or continuous parallel ribs. The average heat transfer coefficient for the ribbed surfaces turned out to be higher than those for the unribbed surface by a factor of up to 2 when the transverse ribs were continuous, and by a factor of up to 3 when they were broken.

Karwa (2003) found that the best heat transfer occurs for the equal pumping power for V-down discrete ribs. Sahu and Bhagoria (2005) investigated experimentally the effect of pitch varying from 10 to 30 by taking the height of the rib to be1.5 mm and duct aspect ratio 8 on the heat transfer coefficient and friction factor for 90˚ broken transverse ribs. It was found that the separation occurred not only at the top edge of the rib but also at the edges at the end of the ribs. This secondary flow interrupted the growth of the boundary layer downstream of the nearby attachment zone in case of 90˚ broken ribs. It was found out that the maximum Nusselt number attained for a pitch of 20 mm and decreased with an increase in roughness pitch. The maximum thermal efficiency of 83.5 % has been found for a 20 mm pitch. Based on experiments, it was found that the maximum thermal efficiency of a roughened solar air heater was of the order of 51 – 83.5 % depending upon the flow conditions.

Aharwal *et al.* (2006) and Aharwal *et al.* (2008) investigated the effect of gap to width ratio (g/e) and gap to position ratio (d/W) in an inclined split rib arrangement in a rectangular duct of a solar air heater as depicted in Figure 6. A gap in the inclined rib arrangement enhanced the heat transfer and friction factor. The increase in the Nusselt number and friction factor, were in the range of 1.48 to 2.59 times and 2.26 to 2.9 times of the smooth duct, respectively. The maximum values of the Nusselt number, friction factor and thermo-hydraulic performance were observed for a gap in the inclined repeated ribs with a relative gap position of 0.25 and relative gap width of 1.0.

3.4.3 Compound roughness

Eiansa-ard and Promvonge (2009) investigated experimentally the combined effect of rib-grooved turbulators on the turbulent forced convection heat transfer and friction characteristics in a rectangular duct. There are three types of rib-groove arrangements: rectangular-rib with triangular-groove, triangular-rib and rectangular-groove and triangular-rib with triangular-groove, which were examined. All rib-groove arrangements significantly enhance the heat transfer rate in comparison with the smooth duct. The thermal enhancement index for the triangular-rib and triangular-groove was achieved and better than that for the rectangular-rib and triangular-groove and triangular-rib and rectangular-groove were around 7% and 4% respectively.

Jaurker *et al.* (2006) investigated the effect of relative roughness pitch, relative roughness height and relative groove position on a heat transfer coefficient and friction factor of rib-grooved artificial

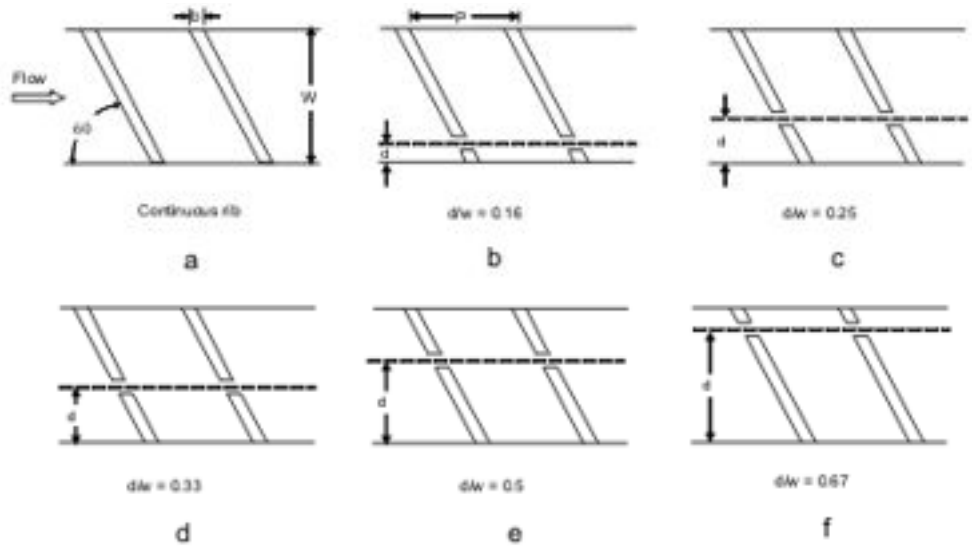

Figure 6: Type and orientation of roughness element investigated by Aharwal *et al.* (2008)

roughness as depicted in Figure 7. The maximum heat transfer was obtained for a relative roughness pitch of about 6, and it was decreased either side of the relative roughness pitch. The optimum condition for heat transfer was found at a groove position to pitch ratio of 0.4 as compared to the smooth duct. As compared to smooth surface, the presence of rib grooved artificial roughness increased the Nusselt number up to 2.7 times, while the friction factor raised up to 3.6 times in the range of parameters investigated.

Layek *et al.* (2007) investigated experimentally the effect of a relative roughness pitch, chamfer angle, relative groove position and relative roughness height on the heat transfer and friction factor for the chamfered rib-groove roughness as depicted in Figure 8. As compared to smooth surface, the chamfer rib-groove roughness resulted in to the increase in the Nusselt number by 3.24 fold and friction factor by 3.78 fold. The maximum heat transfer enhancement occurred for the relative groove pitch of 6 and relative groove position of 0.4. The highest Nusselt number occurred for chamfer angle of 18* but the friction factor increased monotonously with an increase in chamfer angle.

Varun et al. (2008) and Varun et al. (2009) investigated experimentally the thermal performance of a solar air heater having roughness elements as a combination of inclined and transverse ribs on the absorber plate as depicted in Figure 9. It was observed that the best thermal performance occurs for a relative roughness pitch (P/e) of 8.

3.4.4 Small diameter protrusion wires

Prasad and Saini (1988) investigated experimentally the effect of relative roughness pitch (p/e) and relative roughness height (e/D) on the heat transfer coefficient and friction factor of a fully developed turbulent flow in a solar air heater duct with small diameter protrusion wires on the absorber plate. The type and orientation of the geometry is depicted in Figure 10 (Prasad and, Saini 1988). It observed that the average Nusselt number and

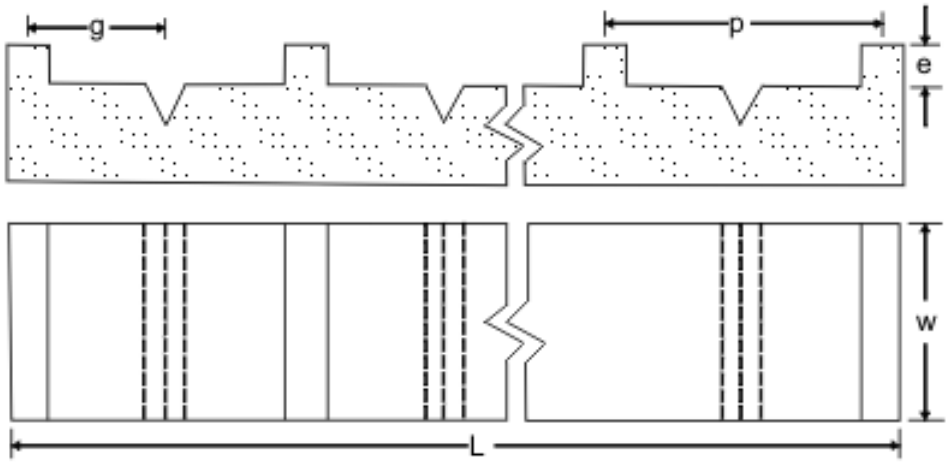

Figure 7: Type and orientation of roughness element investigated by Jaurker *et al.* (2006)

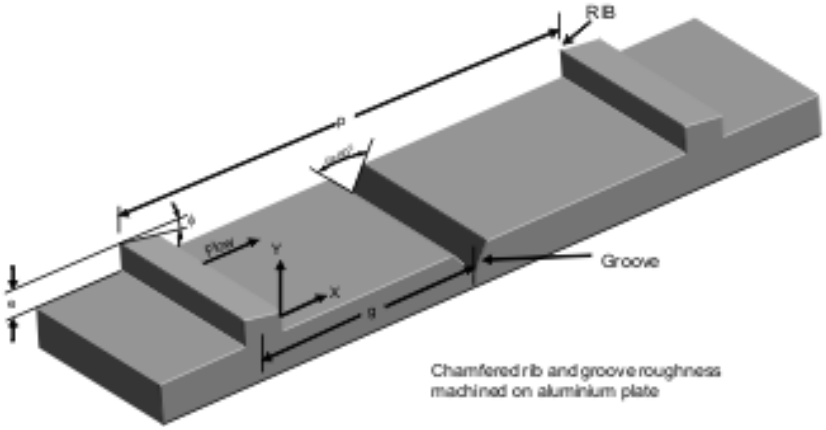

Figure 8: Type and orientation of roughness element investigated by Layek *et al.* (2007)

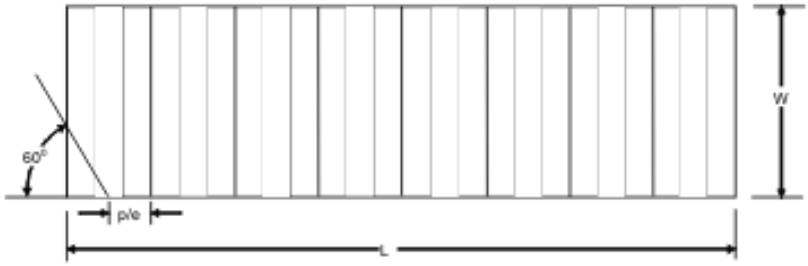

Figure 9: Type and orientation of roughness element investigated by Varun *et al.* (2008)

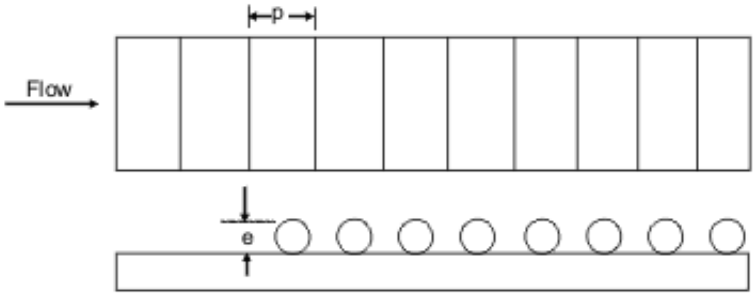

Figure 10: Type and orientation of roughness element investigated by Prasad & Saini (1988)

average friction factor in the roughened duct were as 2.10, 2.24, 2.38 and 3.08, 3.67, 4.25 times that of the smooth duct for relative roughness height of 0.020, 0.027, and 0.033, respectively. It has also been found that increase in the average Nusselt number and average friction factor in the roughened duct were about 2.38, 2.14, 2.01 and 4.25, 3.39, 2.93 times of that of the smooth duct for a relative roughness pitch of 10, 15, and 20, respectively. The maximum enhancement in the heat transfer coefficient and friction factor were as 2.38 and 4.25 times than that of smooth duct respectively.

Gupta et al. (1993) investigated the effect of a duct aspect ratio and relative roughness height at a relative roughness pitch of 10, with the Reynolds number range of 3 000 to 18 000, and developed the correlations for heat transfer and friction factor for transverse rib roughness on the absorber plate. It has been found that the behaviour of the Stanton number in a transitionally rough flow region was different from its behaviour in a fully rough flow region. Correlations for transitionally rough flow regions have been developed for the range of investigation. These correlations showed good agreement between the predicted and experimental values of the heat transfer coefficient and friction factor.

Verma and Prasad (2000) have investigated the effect of similar geometrical parameters of circular wire ribs on heat transfer and friction factor. It was observed that the Nusselt number varied from 1.25 to 2.08 times that of a smooth duct within the range of parameters investigated.

3.4.5 Expanded wire mesh

Saini and Saini (1997) investigated experimentally the effect of expanded metal mesh geometry as depicted in Figure 11 for fully developed turbulent

flow in a rectangular duct with a large aspect ratio (11:1). The effect of expanded metal mesh geometry [i.e. relative long way length of mesh (L/e), relative short way length of mesh (S/e) and relative roughness height of mesh (e/D)] on the heat transfer coefficient and friction factor was investigated. The maximum Nusselt number and friction factor were found corresponding to relative long way length of mesh of 46.87 and 71.87 respectively for all the values of relative short way length of mesh investigated. The maximum Nusselt number and friction factor occurred for relative short way length of mesh of 25 and 15 respectively. The maximum enhancement in Nusselt number and friction factor values were reported of the order of 4 and 5 times to the smooth absorber plate respectively.

Paswan and Sharma (2009) studied experimentally, the thermal performance of wire-screen mesh (metal) as artificial roughened on the underside of its absorber plate. Thermal performance of a solar air heater enhanced considerably by roughing the absorber plate with wire screen metal mesh, and this enhancement was a strong function of geometrical parameters (such as diameter of wire and pitch) and operating parameters (mass flow rate, insulation and inlet temperature). Decreasing values of wire-pitch, leads to increasing value of thermal performance of solar air heater.

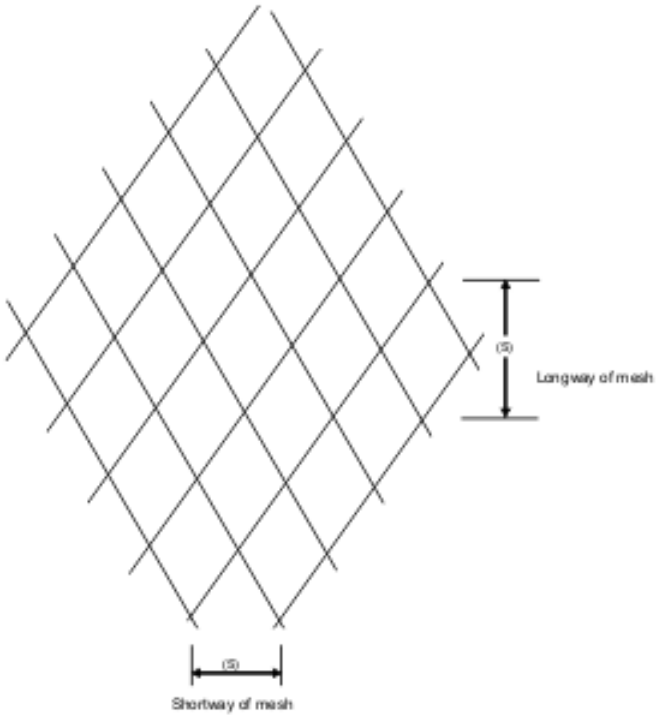

Figure 11: Type and orientation of roughness element investigated by Saini & Saini (1997)

3.4.6 Chamfered ribs

Karwa *et al.* (1999) and Karwa *et al.* (2001) investigated experimentally the effect of repeated chamfered rib-roughness on one broad wall and the duct aspect ratio on the heat transfer coefficient and fluid friction as depicted in Figure 12. It has been observed that the presence of chamfered ribs at one broad wall of the duct yields up to about two-fold and three-fold increase in the Stanton number and the friction factor, respectively, as compared to the smooth duct. The highest heat transfer and also the highest friction factor occur for 15° chamfered ribs. The minima of the heat transfer function occur at a roughness Reynolds number of about 20. The heat transfer function increases with the increase in the aspect ratio from 4.65 to 9.66, and the roughness function decreases with the increase in the aspect ratio from 4.65 to 7.75. Thereafter, both the functions attain nearly a constant value.

There was an appreciable increase in the thermal efficiency (10 to 40 %) of the solar air heaters with chamfered-rib roughened absorber plate due to the enhancement in the Nusselt number of the

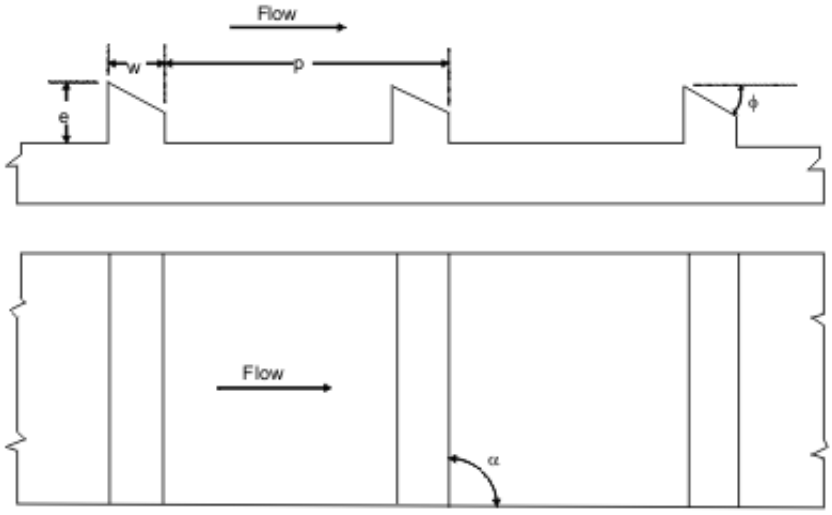

Figure 12: Type and orientation of roughness element investigated by Karwa *et al.* (1999)

order of 50 to 120% over the smooth absorber plate. The enhancement in the Nusselt number, friction factor and thermal efficiency were found to be strong functions of the relative roughness height. The greatest enhancement was observed for the air heater with the highest relative roughness height.

3.4.7 Wedge shaped ribs

Bhagoria *et al.* (2002) has performed experiments in order to find out the effect of relative roughness height, relative roughness pitch and wedge angle on the heat transfer and friction factor in a solar air heater roughened duct having wedge shaped rib roughness as depicted in Figure 13. It has been observed that the maximum heat transfer occurred for a relative roughness pitch of about 7.57, while the friction factor decreased as the relative roughness pitch increased. A maximum enhancement of heat transfer occurred at a wedge angle of about 10°. As compared to the smooth duct, the presence of ribs yielded a Nusselt number up to 2.4 times while the friction factor raised up to 5.3 times for the range of parameters investigated.

3.4.8 Arc shaped ribs

Saini and Saini (2008) investigated experimentally the effect of relative roughness height (e/d) and relative angle of attack (α/90) of arc-shape parallel wire on the heat transfer coefficient and friction factor as depicted in Figure 14 and Figure 15. The maximum enhancement in the Nusselt number was obtained as 3.80 times corresponding to the relative arc angle (α/90) of 0.3333 at relative roughness height of 0.0422. However, the increment in the friction factor corresponding to these parameters was found to be only 1.75 times.

Kumar and Saini (2009) used Computational Fluid Dynamics for analyzing the performance of a solar air heater duct provided with artificial roughness in the form of thin circular wire in arc shaped geometry. Overall enhancement ratio with a maximum value of 1.7 has been found for the roughness geometry corresponding to the relative arc angle (□/90) of 0.3333 at relative roughness height of 0.0426 for relative roughness pitch of 10. The overall enhancement ratio (OER) given by Wang and Sunden (2002) is as below.

$$OER = \frac{Nu_r / Nu_s}{\left(f_r / f_s \right)^{1/3}} \quad (3.1)$$

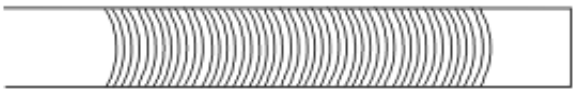

Figure 14: Type and orientation of roughness element investigated by Saini and Saini (2008)

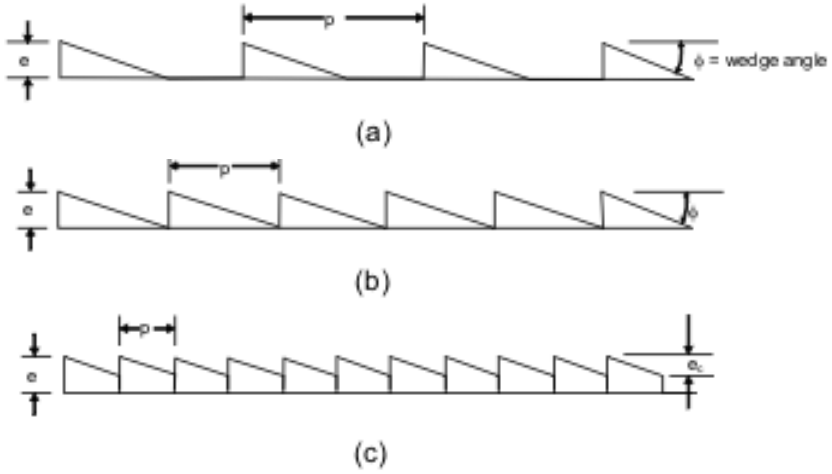

Figure 13: Type and orientation of roughness element investigated by Bhagoria *et al.* (2002)

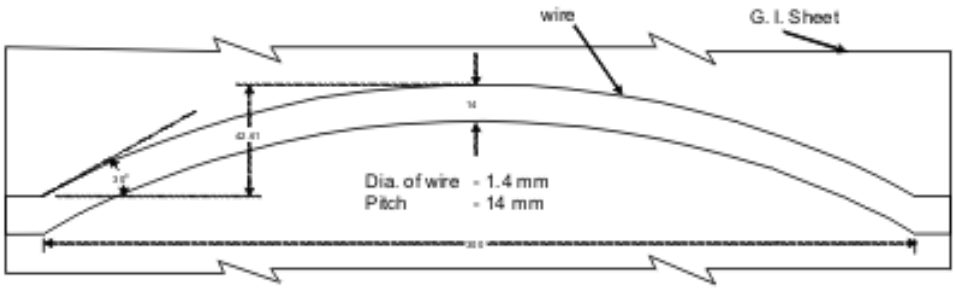

Figure 15: Type and orientation of roughness element investigated by Saini and Saini (2008)

3.4.9 Dimple

Saini and Verma (2008) investigated the effect of relative roughness height (e/D) and relative roughness pitch (P/e) of dimple-shape roughness geometry on heat transfer and friction factor as depicted in Figure 16. It was found that heat transfer could be enhanced considerably as a result of providing dimple-shape roughness geometry on the absorber plate of a solar air heater duct.

The maximum value of the Nusselt number was found to correspond to relative roughness height of 0.0379 and relative roughness pitch of 10, while minimum value of the friction factor was found corresponding to relative roughness height of 0.0289 and relative pitch of 10. It was concluded that the roughness parameters of the geometry can be selected by considering the net heat gain and corresponding power required to propel air through the duct.

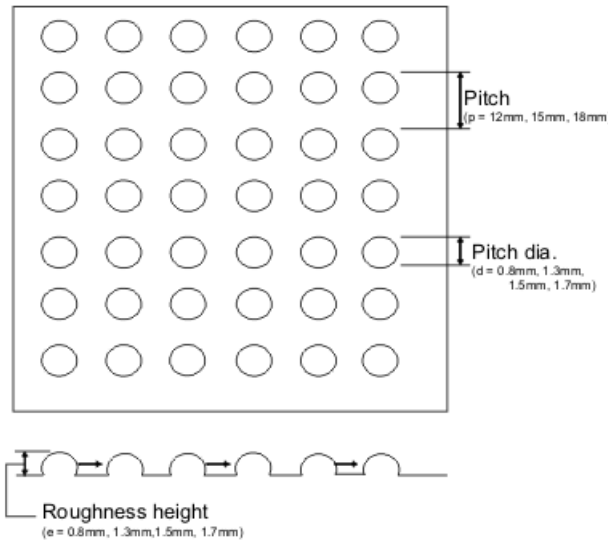

Figure 16: Type and orientation of roughness element investigated by Saini and Verma (2008)

3.4.10 Metal grit ribs

Karmare and Tikekar (2007) investigated experimentally the effect of metal ribs of the circular cross section in a staggered manner to form a defined grid as depicted in Figure 17. The effect of the relative roughness height of grit (e/D), relative roughness pitch of grit (P/e), relative length of grit (l/s) on the heat transfer and friction factor were investigated. As compared to a smooth surface, the presence of metal grit ribs on the collector surface of the duct yielded up to two-fold enhancement in the Nusselt number and three-fold enhancement in the friction factor. The highest heat transfer was found for l/s = 1.72, e/D = 0.044 and P/e = 17.5, where the highest friction factor was found for l/s = 1.72, e/D = 0.044 and P/e = 12.5.

Optimum performance was observed for l/s = 1.72, e/D = 0.044 and P/e = 17.5 for the range of parameters studied. Enhancement in the Nusselt number was found to be 187% and the friction factor by 213 % as compared with a smooth surface.

3.4.11 Inverted u-shaped turbulators

Bopche and Tandale (2009) investigated experimentally the effect of the inverted U-shaped turbulators on the absorber surface of an air heater duct on the heat transfer coefficient and friction factor. The inverted U-shaped turbulator showed appreciable heat transfer enhancement even at a low Reynolds number (Re < 5000) where ribs were inefficient. At the Reynolds number, Re = 3800, the maximum enhancement in the Nusselt number and friction factor were of the order of 2.388 and 2.50, respectively. The maximum enhancement in the Nusselt number and friction factor values compared to the smooth duct were of the order of 2.82 and 3.72, respectively. The turbulence generated only in the viscous sub-layer region of the boundary layer resulted in better thermo-hydraulic performance i.e. maximum heat transfer enhancement at an affordable friction penalty.

3.5 Aspect ratio

Karwa (1999) has also presented the detailed experimental evidence of this effect. He compared the heat transfer and friction factor characteristics for the duct of the aspect ratio 4.8 and 7.75. He found that the Stanton number ratio, St_r / St_s, decreased

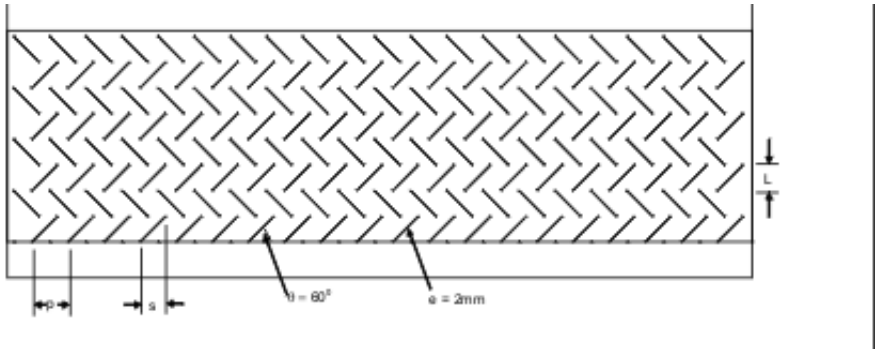

Figure 17: Type and orientation of roughness element investigated by Karmare and Tikekar (2007)

by about 5% with an increase in the aspect ratio from 4.8 to 7.75. The friction factor ratio f_r / f_s, increased by about 20% for the corresponding flow conditions.

Karwa (2003) also compared the results for the aspect ratio 5 and 7.5 for asymmetrically heated rectangular ducts with ribs on the heated wall in the transverse, inclined, V-continuous and V-discrete pattern. The average increase in the friction factor ratio f_r / f_s is about 10.48%, with an increase of aspect ratio from 5 to 7.5. The Stanton number ratio St_r / St_s decreased by 5.12 % with an increase in aspect ratio from 5 to 7.5. Based on the experimental investigation carried out by various investigators, the developed correlations for the Nusselt number and friction factor are also presented in Table 3 within the range of operating parameters.

Table 3: Correlations developed for heat transfer and friction factor for different roughness geometries used in solar air heater duct

Investigator(s)	*Types of roughness*	*Range of operating parameters*	*Results in the form of Correlations*
Karwa *et al.* (1999)	Chamfered ribs	P/e =4.5 to 8.5 e/D=0.014 to 0.032 ϕ= -15^0 to +18^0 Re = 3000 to 20,000	For7=e^+<20 $R = 1.66e^{-0.0078\phi}(W/H)^{-0.4}(P/e)^{2.695} \times Exp\left[-0.762\{\ln(p/e)\}^2\right](e^+)^{-0.075}$ When W/H >7.75 use W/H=7.75 $g = 103.77e^{-0.006\phi}(W/H)^{0.5}(p/e)^{-2.56} \times Exp\left[0.7343\{\ln(p/e)\}^2\right](e^+)^{-0.31}$ When W/H >10 use W/H=10 For 20=e^+=60 $R = 1.325\ e^{-0.0078\ \phi}(W/H)^{-0.4}(p/e)^{2.695} \times Exp\left[-0.762\ \{\ln(p/e)\}^2\right]$ When W/H >7.75 use W/H=7.75 $g = 32.2e^{-0.006\ \phi}(W/H)^{0.5}(p/e)^{-2.56} \times Exp\left[0.7343\ \{\ln(p/e)\}^2\right](e^+)^{0.08}$ When W/H >10 use W/H=10 $R = \sqrt{(2/f)} + 2.5\ln(2e/D) + 3.75$ $g = \{f/(2St) - 1\}\sqrt{(2/f)} + R$
Layek *et al.* (2007)	Chamfered rib-groove	p/e= 4.5 to 10 e/D= 0.022 to 0.04 g/p= 0.3 to 0.6 ϕ= 5^0 to 30^0 Re= 3000 to 21000	$f_r = 0.00245\ (\mathrm{Re})^{-0.124}(e/D)^{0.365}(p/e)^{4.32}(g/p)^{-1.124} \times [Exp\ (0.005\ \phi)] \times [Exp\ \{-1.09\ (\ln(p/e))^2\}] \times [Exp\ \{-0.68\ (\ln(g/p))^2\}]$ $Nu_r = 0.00225\ (\mathrm{Re})^{0.92}(e/D)^{0.52}(p/e)^{1.72}(g/p)^{-1.21}(\phi)^{1.24} \times [Exp\ \{-0.22\ (\ln\phi)^2\}][Exp\ \{-0.46\ (\ln(p/e))^2\}] \times [Exp\ \{-0.74\ (\ln(g/p))^2\}]$
Jaurker *et al.* (2006)	Rib-groove	p/e= 4.5 to 10 e/D= 0.0181 to 0.0363 g/p= 0.3 to 0.7 Re= 3000 to 21000	$f_r = 0.001227\ (\mathrm{Re})^{-0.199}(e/D)^{0.585}(p/e)^{7.19}(g/p)^{0.645} \times [Exp\ \{-1.854\ (\ln(p/e))^2\}] \times [Exp\ \{1.513\ (\ln(g/p))^2 + 0.8662\ (\ln(g/p))^3\}]$ $Nu_r = 0.002062\ (\mathrm{Re})^{0.936}(e/D)^{0.349}(p/e)^{3.318} \times [Exp\ \{-0.868\ (\ln(p/e))^2\}] \times (g/p)^{1.108} \times [Exp\ \{2.486\ (\ln(g/p))^2 + 1.406\ (\ln(g/p))^3\}]$

Prasad and Saini (1988)	Small diameter protrusion wires	P/e =10 to 20 e/D =0.022 to0.033 R_e = 5000 to 50000	$\overline{f} = \frac{(W + 2H) f_s + W f_r}{2(W + H)}$ $f_r = \frac{2}{[0.95(P/e)^{0.53} + 2.5 \log_e(D/2e) - 3.75]^2}$ $\overline{S_t} = \frac{f/2}{1+\sqrt{(f/2)[4.5(e^+)^{0.28} P_r^{0.57} - 0.95(P/e)^{0.53}]}}$ $\overline{Nu} = \overline{S}_t R_e P_r$
Karwa R. (2003)	V-continuous and V-discrete	P/e =10 e/D=0.0467 to 0.05 $\alpha = 90^0$ and 60^{0+} Re = 2800 to 15000	$R = a(e^+)^b$ $g = a_1 + b_1(e^+) + c_1(e^+)^2$ Value of a, b, a_1, b_1, and c_1 will get from table (4)
Momin *et al.* (2002)	V-shaped	P/e =10 e/D=0.02 to 0.034 $\alpha = 30^0$ to 90^0 Re = 2500 to 18,000	$f_r = 6.266 \times (\mathrm{Re})^{-0.425} (e/D)^{0.565} (\alpha/60^0)^{-0.093} \times Exp\left[-0.719 \times (\ln \alpha/60^0)^2\right]$ $Nu_r = 0.067 \times (\mathrm{Re})^{0.888} (e/D)^{0.424} (\alpha/60^0)^{-0.077} \times Exp\left[-0.782 \times (\ln \alpha/60^0)^2\right]$
Gupta *et al.* (1993)	Transverse wire roughness	p/e=10 e/ D= 0.018 to 0.052 W/H= 6.8 to 11.5 Re= 3000 to 18000	$f_r = 0.06412 (e/D)^{0.019} (W/H)^{0.237} (\mathrm{Re})^{-0.185}$ For $e^+<35$ $Nu_r = 0.000824(e/D)^{-0.178}(W/H)^{0.288}(\mathrm{Re})^{1.062}$ For $e^+\geq 35$ $Nu_r = 0.00307 (e/D)^{-0.469} (W/H)^{0.245} (\mathrm{Re})^{0.812}$ where $e^+ = (e/D)\mathrm{Re}(f/2)^{0.5}$
Saini and Saini (1997)	Expanded metal mesh	e/D= 0.012 to0.0390 L/e= 25.00 to 71.87 S/e= 15.62 to 46.87 Re= 1900 to 13000	$f_r = 0.815(\mathrm{Re})^{-0.361}(L/e)^{0.266}(S/10e)^{-0.190}(10e/D)^{0.591}$ $Nu_r = 4.0 \times 10^{-4} \mathrm{Re}^{1.22} (e/D)^{0.625} (S/10e)^{2.22} \times \left[Exp\left\{-1.25(\ln(S/10e))^2\right\}\right] \times (L/10e)^{2.66} \left[Exp\left\{-0.824(\ln(L/10e))^2\right\}\right]$
Bhagoria *et al.* (2002)	Wedge shaped rib	P/e =$60.17\psi^{-1.0264}$ to 12.12 e/D=0.015 to 0.033 $\psi = 8^0$ to 15^0 Re= 3000 to 18000	$f_r = 12.44(\mathrm{Re})^{-0.18}(e/D)^{0.99}(p/e)^{-0.52}(\Psi/10)^{0.49}$ $Nu_r = 1.89 \times 10^{-4} (\mathrm{Re})^{1.21} (e/D)^{0.426} (p/e)^{2.94} \times \left[Exp\left\{-0.71(\ln(p/e))^2\right\}\right] \times (\Psi/10)^{-0.018} \times \left[Exp\left\{-1.50(\ln(\Psi/10))^2\right\}\right]$

Saini and Saini (2008)	Arc shaped wire roughness	P/e= 10 e/D= 0.0213 to 0.0422 a/.90= 0.3333 to 0.6666 Re= 2000 to 17000	$f_r = 0.14408\,(\mathrm{Re})^{-0.17103}\left(e/D\right)^{0.1765}\left(\alpha/90\right)^{0.1185}$ $Nu_r = 0.00104(\mathrm{Re})^{1.3186}\left(e/D\right)^{0.3772}\left(\alpha/90\right)^{-0.1198}$
Saini and Verma (2008)	Dimple-shape roughness	P/e= 8 to 12 e/D= 0.0189 to 0.038	$f_r = 0.642\,(\mathrm{Re})^{-0.423}\left(P/e\right)^{-0.465}\left[\exp\,(0.054)(\log\left(P/e\right))^2\right]$ $\times\left(e/D\right)^{-0.0214}\left[\exp\,(0.840)(\log\left(e/D\right))^2\right]$
		Re= 2000 to 12000	$Nu_r = 5.2\times10^{-4}(\mathrm{Re})^{1.27}\times\left(P/e\right)^{3.15}\times\left(e/D\right)^{0.033}$ $\times\left[\exp(-2.12)(\log(P/e))^2\right]\times\left[\exp(-1.30)(\log(e/D))^2\right]$
Varun *et al.* (2008)	Combination of inclined and transverse ribs V	P/e= 3 to 8 e/D= 0.030 Re= 2000 to 14000	$f_r = 1.0858\,(\mathrm{Re})^{-0.3685}\times\left(P/e\right)^{0.0114}$ $Nu_r = 0.0006\,(\mathrm{Re})^{1.213}\times\left(P/e\right)^{0.0104}$
Karmare and Tikekar (2007)	Metal grit rib roughness	P/e= 12.5 to 36 e/D= 0.035 to 0.044 l/s= 1 to 1.72 Re= 4000 to 17000	$f_r = 15.55\,(\mathrm{Re})^{-0.26}\times\left(e/D\right)^{0.91}\times\left(l/s\right)^{-0.27}\times\left(P/e\right)^{-0.51}$ $Nu_r = 2.4\times10^{-3}(\mathrm{Re})^{1.3}\left(e/D\right)^{0.42}\left(l/s\right)^{-0.146}\left(P/e\right)^{-0.27}$
Bopche and Tandale (2009)	Inverted U-shaped turbulators	P/e= 6.667 to 57.14 e/D= 0.0186 to 0.03986 Re= 3800 to 18000	$f_r = 1.2134\times\mathrm{Re}^{-0.2076}\times\left(P/e\right)^{-0.4259}\times\left(e/D\right)^{0.3285}$ $Nu_r = 0.5429\times\mathrm{Re}^{0.7054}\times\left(P/e\right)^{-0.1592}\times\left(e/D\right)^{0.3619}$

Table 4: Coefficient for roughness and heat transfer functions for V-continuous and V-discrete ribs *(Karwa, 2003)*

Roughness	*a*	*b*	a_1	b_1	C_1
Inclined	3.7135	0.12770	12.765	-0.05095	0.000506
V-up continuous	3.5080	0.12195	12.382	-0.04547	0.000408
V-down continuous	3.4590	0.13048	12.502	-0.11609	0.001239
V-up discrete	4.0917	0.16083	11.249	-0.13120	0.001479
V-down discrete	3.5341	0.19102	11.070	-0.14900	0.001757

4. Colburn factor (j factor) and friction factor (f factor)

The enhanced surface on one hand, provides a greater heat transfer coefficient, but also leads to increased fluid flow friction and pressure drop. Sometimes, the benefits gained from heat transfer enhancement are not great enough to offset the increased friction losses. Clearly, then the performance goal is to gain maximum enhancement of heat transfer with minimum penalty on pumping power. The criterion of selecting good geometries done on the basis of comparing the heat transfer coefficients or dimensionless heat transfer parameters (i.e. Nusselt number, Stanton number etc) is not good enough. So, performance data for an enhanced surface are shown as curves of the Colburn factor (J) and the friction factor (f) plotted versus Reynolds number (Re). The curves for J and f plotted vs. Re tend to vary over a wide range, in magnitude as well as slope. Various steps involved in the evaluation have been explained below:

$$P_r = \frac{\mu}{C_p \cdot K} \tag{4.1}$$

$$S_t = \frac{N_u}{R_e . P_r} \tag{4.2}$$

$$J = S_t \cdot (P_r)^{2/3} \quad (4.3)$$

The value of the heat transfer coefficient and friction factor for roughened solar air heaters has been determined from the correlations developed for heat transfer and friction factors by several investigators as given in Table. 3. The set of system operating parameters (shown in bracket of Table.3, column 3) for particular roughness geometry at which thermo hydraulic behaviour has been reported best, is selected for the analysis.

Figure 18 depicts the variation of the Colburn factor (J) with the Reynolds number, for various considered geometries (rough and smooth). The Colburn factors for all the geometries are higher than that of the smooth surface for the entire range of Re, except Gupta *et al.* (1993) and Saini and Verma (2008) up to Re around 4000.

It has been observed that the maximum value of the Colburn factor has been achieved for Bopche and Tandale (2009) at Re 3000, but at Re 24000 the maximum value of the Colburn factor has been observed for Saini and Saini (2008). The Colburn factor decreases with an increase in Re in case of smooth surface, V-continuous, V-discrete, rib-grooved, chamfered rib-grooved, small diameter protrusion wire and Inverted U-shaped turbulators. But the Colburn factor increases with increase in Re in case of dimple, transverse wire roughness, combination of inclined and transverse ribs, metal grit rib roughness, arc shaped wire roughness, expanded wire mesh, wedge shaped rib.

Figure 19 depicts the variation of friction factors

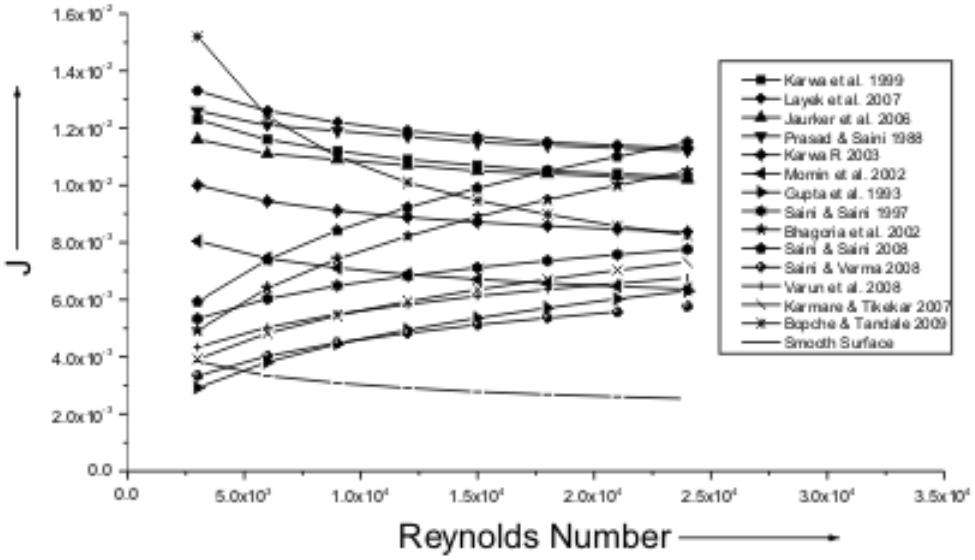

Figure 18: Colburn factor (j factor) versus Reynolds Number

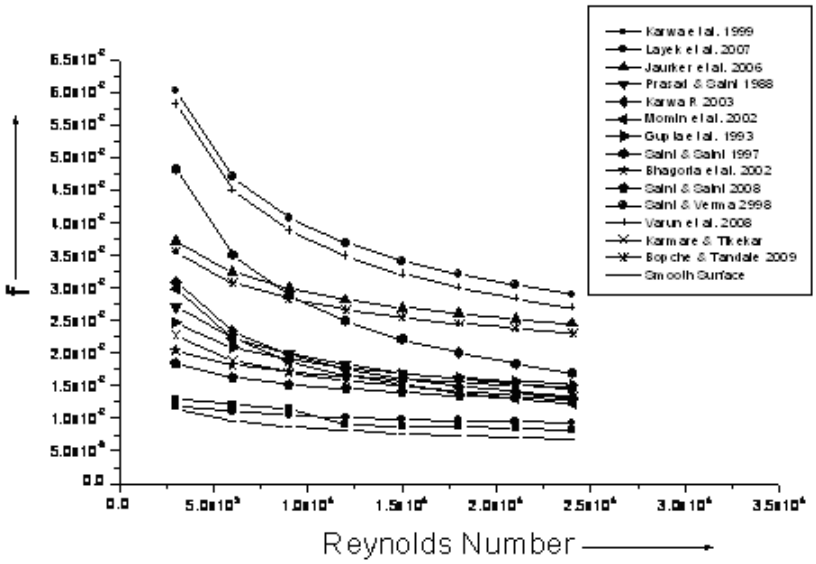

Figure 19: Friction factor (f factor) versus Reynolds Number

with the Reynolds number. It is seen that the friction factor decreases with increase in Re for all types of roughness geometries, and friction factor of any considered rough surface is always higher than the smooth surface. The friction factor, among the considered geometries, in general increases in the following sequence: smooth surface, chamfered rib-groove, chamfered rib, arc shaped wire, wedge shaped rib, metal grit rib, transverse wire roughness, small diameter protrusion wire, V-continuous and V-discrete, Inverted U-shaped, rib-groove, expanded wire mesh, inclined and transverse ribs and dimple. Finally, one can conclude that there is not a single roughness geometry which gives the best result for the whole range of Re.

5. Conclusions

This paper reviews the investigation carried out by various researchers in order to enhance the heat transfer and friction factor by the use of artificial roughness of different shapes, sizes and orientations. It can be concluded that there is a considerable enhancement in heat transfer with little penalty of friction.

Correlations developed for heat transfer and friction factor for solar air heater ducts having artificial roughness of different geometries for different investigators are also shown in tabular form. These correlations can be used to predict the thermal efficiency, effective efficiency and then hydraulic performance of artificial roughened solar air heater ducts.

The Colburn factors are improved by using roughened geometries in the duct of the solar air heater but friction factors are also increased. A solar air heater having a dimple has roughness elements, and is found to have a maximum value of friction factor in all the range of Reynolds number.

This paper is very helpful for researchers in carrying out the experimental and numerical investigations to find out and optimize the new element geometries for the maximum enhancement of heat transfer.

Nomenclature

D	equivalent diameter of the air passage (m)
d/w	relative gap position
e	height of roughness element (m)
e^+	roughness Reynolds number
e/D	relative roughness height
f_r	friction factor of roughened duct
f_s	friction factor of smooth duct
g	heat transfer function (g-function)
g/e	relative gap width
g/p	groove position to pitch ratio
G	momentum heat transfer function
G (e^+)	heat transfer roughness function
H	height of duct (m)
l/s	relative length of metal grit
L/e	relative long way length
S/e	relative short way length
Nu	Average Nusselt number
Nu_r	Nusselt number for roughened duct
Nu_s	Nusselt number for smooth duct
p_r	Prandtl number
p	oughness pitch (m)
p/e	relative roughness pitch
R	roughness function
Re	Reynolds number
R (e^+)	Reynolds roughness number
St	average Stanton number
St_r	Stanton number for roughened duct
St_s	Stanton number for smooth duct
U^+	dimensionless velocity
Y^+	dimensionless distance

Greek symbols

α	rib angle of attack
$\alpha/90$	relative angle of attack
ϕ	chamfer angle
Ψ	wedge angle

References

Aharwal, K.R. Gandhi, B.K. and Saini, J.S., (2006). Effect of gap in inclined ribs on the performance of artificially roughened solar air heater duct, *Advances in Energy Research,* pp.144-150.

Aharwal, K.R. Gandhi, B.K. and Saini, J.S., (2008). Experimental investigation on heat transfer enhancement due to a gap in an inclined continuous rib arrangement in a rectangular duct of solar air heater, Renewable energy, 33, pp. 585 – 596.

Bhagoria, J.S. Saini, J.S. and Solanki, S.C., (2002). Heat transfer co-efficient and friction factor correlation for rectangular solar air heater duct having transverse wedge shaped rib roughness on the absorber plate, *Renewable Energy*, 25, pp. 341 – 369.

Bopche S.B. and Tandale M.S., (2009). Experimental investigation on heat transfer and friction characteristics of a turbulator roughened solar air heater duct, *International Journal of heat and Mass Transfer,* 52, pp. 2834 – 2848.

Dipprey, D.F. and Sabersky, R.H., (1963) Heat and momentum transfer in smooth and rough tubes at various Prandtl numbers, *Int. J. Heat Mass Transfer*, 6, pp. 329 – 353.

Eiamsa-ard, S. and Promvonge, P., (2009). Thermal characteristics of turbulent rib-grooved channel flows, Int. Comm. *Heat Mass Transfer*, 36, pp. 705 – 711.

Gee, D.L. and Webb, R.L., (1980). Forced convective heat transfer in helically rib- roughened tubes, *Int. J. Heat Mass Transfer*, 21, pp. 1127 -1136.

Gupta, D. Solanki, S.C. and Saini, J.S., (1993). Heat and fluid flow in rectangular solar air heater ducts having transverse rib roughness on absorber plate, *Solar Energy*, 51, pp. 31-37.

Jaurker, A.R. Saini, J.S. and Gandhi, B.K., (2006). Heat transfer and friction characteristics of rectangular solar air heater duct using rib-grooved artificial roughness, *Solar Energy*, 80, pp. 895 – 907.

Karmare, S.V. and Tikekar, A.N., (2007). Heat transfer and friction factor correlation for artificially roughened duct with metal grit ribs, *Int. Journal of Heat Mass Transfer*, 50, pp. 4342 – 4351.

Karwa, R. Solanki, S.C. and Saini, J.S., (1999) Heat transfer coefficient and friction factor correlations for the transitional flow regimes in rib-roughened rectangular duct, *Int. Journal of Heat Mass Transfer,* 42, pp. 1597 -1615.

Karwa, R. Solanki, S.C. and Saini, J.S., (2001). Thermo-hydraulic performance of solar air heaters having integral chamfered rib roughness on absorber plate, *Energy*, 26, pp. 161 – 176.

Karwa, R., (2003). Experimental studies of augmented heat transfer and friction in asymmetrically heated rectangular ducts with ribs on the heated wall in transverse, inclined, V-continuous and V-discrete pattern, *Int. Comm. Heat Mass Transfer*, 30, pp. 241 – 250.

Kumar, S. and Saini, R.P., (2009). CFD based performance analysis of a solar air heater duct provided with artificial roughness*, Renewable Energy*, 34, pp. 1285 – 1291.

Laohalertdecha, S. Naphon, p. and Wongwises, S., (2007). A review of electro hydrodynamic enhancement of heat transfer, *Renewable and Sustainable Energy Reviews,* 11, pp. 858 – 876.

Layek, A. Saini, J.S. and Solanki, S.C., (2007). Heat transfer and friction characteristics for artificially roughened duct with compound turbulators, *International Journal of Heat and Mass Transfer,* 50, pp. 4845 – 4854.

Momin, A-M E. Saini, J.S. and Solanki, S.C., (2002). Heat transfer and friction in solar air heater duct with V-shaped rib roughness on absorber plate, *Int. Journal of Heat and Mass Transfer,* 45, pp. 3383 – 3396.

Muluwork, K.B. Saini, J.S. and Solanki, S.C., (1998). Studies on discrete RIB roughened solar air heater, In: Proceedings of National Solar Energy Convention, Roorkee, pp. 75 -84.

Nikuradse, J., (1950). Law of flow in rough pipes, NACA, Technical Memorandom, 1292.

Paswan, M.K. and Sharma, S.P., (2009). Thermal performance of wire-mesh roughened solar air heaters, Arab Research Institute in Science & Engineering, 1, pp. 31 – 40.

Prasad, B.N. and Saini, J.S., (1988). Effect of artificial roughness on heat transfer and friction factor in solar air heater, *Solar Energy*, 41, pp. 555 – 560.

Prasad, B.N. and Saini, J.S., (1991). Optimal thermo hydraulic performance of artificial roughness solar air heater, *Solar Energy*, 47, pp 91 – 96.

Reddy, T.A. and Gupta, C.L., (1980). Generating applications design data for solar air heating systems, *Solar Energy,* 25, pp. 527 – 530.

Sahu, M.M. and Bhagoria, J.L., (2005). Augmentation of heat transfer co-efficient by using 90° broken transverse rib on absorber plate of solar air heater, *Renewable Energy*, 30, pp. 2057 – 2073.

Saini, R.P. & Verma, J., (2008). Heat transfer and friction correlations for a duct having dimple shape artificial roughness for solar air heater, *Energy*, 33, pp. 1277-1287.

Saini, R.P. and Saini, J.S., (1997) Heat transfer and friction factor correlations for artificially roughened duct with expanded metal mesh as roughness element, *Int. Journal of Heat Mass Transfer*, 40, pp. 973 – 986.

Saini, S.K. and Saini, R.P., (2008). Development of correlations for Nusselt number and friction factor for solar air heater with roughened duct having arc-shaped wire as artificial roughness, *Solar Energy*, 82, pp. 1118 – 1130.

Varun, Patnaik, A. Saini, R.P. Singal, S.K. and Siddhartha., (2009). Performance prediction of solar air heater having roughened duct provided with transverse and inclined ribs as artificial roughness, *Renewable Energy*, pp. 1-9, Article in Press.

Varun, Saini, R.P. and Singal, S.K., (2008). Investigation on thermal performance of solar air heaters having roughness elements as a combination of inclined and transverse ribs on the absorber plate, *Renewable Energy*, 33, pp. 1398 – 1405.

Verma, S.K. and Prasad, B.N., (2000. Investigation for the optimal thermo hydraulic performance of artificially roughened solar air heaters, *Renewable Energy*, 20, pp.19 – 36.

Wang, L. and Sunden, B., (2002). Performance comparison of some tube inserts, *Int. Comm. Heat Mass Transfer*, 29, pp. 45 – 56.

Webb, R.L. Eckert, ERG. and Goldstein, R.J., (1971). Heat transfer and friction in tubes with repeated-rib roughness, *Int. Journal Heat Mass Transfer*, 14, pp. 601 – 617.

Received 5 March 2009; revised 2 December 2009